SUPPLEMENTAL MATERIAL

Perry et al., https://doi.org/10.1084/jem.20171435

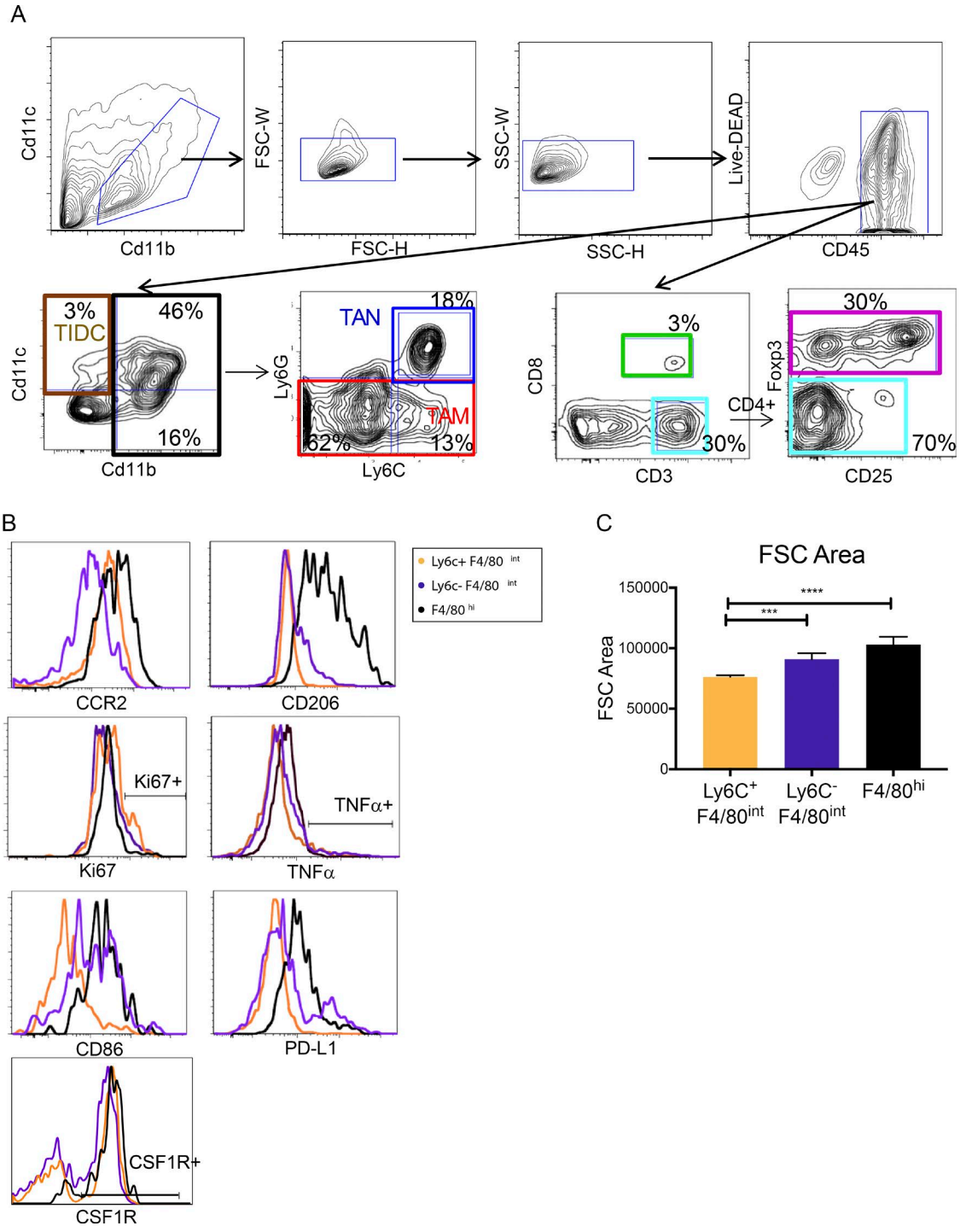

Figure S1. **Analysis of immune cell composition and myeloid heterogeneity in end point tumors.** Related to Fig. 1. **(A)** Representative gating strategy of Fig. 1 (A, D, and E). T regulatory cells were defined as $CD45^+$ $CD3^+$ $CD4^+$ $Foxp3^+$, distinguished from non–T regulatory cell CD4s by Foxp3 expression. CD8 T cells were defined as $CD45^+$ $CD3^+$ $CD8^+$. TAMs were defined as $CD45^+$ $CD11b^+$ $Ly6G^-$, distinct from TANs ($CD45^+$ $CD11b^+$ $Ly6G^+$). Tumor-infiltrating DCs (TIDCs) were defined as $CD45^+$ $CD11c^+$ $CD11b^-$ $Ly6G^-$. Indicated percentages are averaged from two representative experiments. **(B)** Histograms from Fig. 1 E showing CCR2, CD206, Ki67, TNF-α, CD86, PD-L1, and CSF-1R TAM phenotypes from end point (1 cm^3) tumors, as shown by concatenated plots of each individual mouse tumor. Data are from one experiment and are representative of three experiments ($n = 6$ each group). **(C)** Mean flow cytometry (FSC) area (±SEM) histogram from Fig. 1 D from end point (1 cm^3) tumors. Significant differences between groups were determined by one-way ANOVA with Holm-Sidak multiple comparisons correction. Data are from one experiment and are representative of three experiments ($n = 6$ each group). ***, $P < 0.005$; ****, $P < 0.001$.

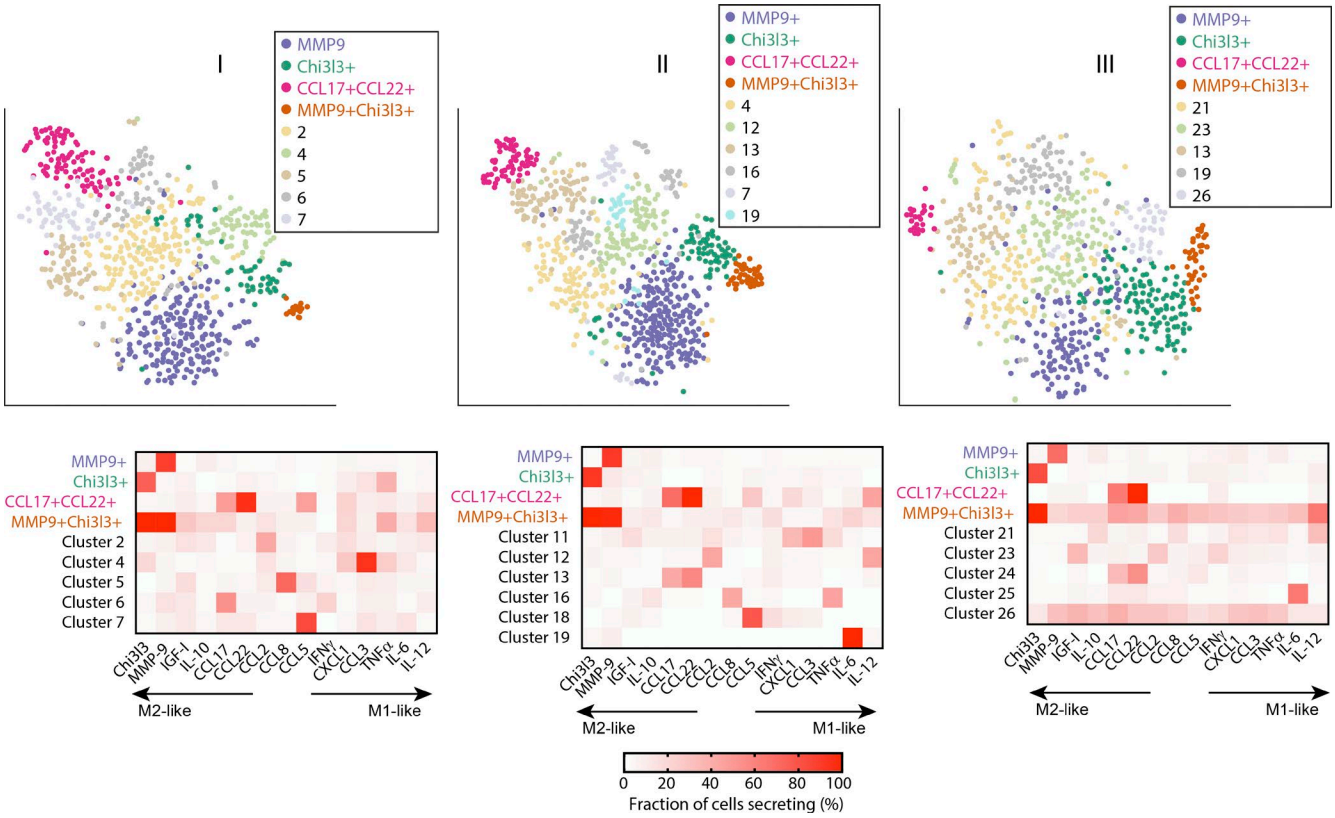

Figure S2. **Single-cell secretion profiling of TAMs from end point tumors.** Related to Fig. 2. 2D t-SNE representation of single TAM cell projected from 15-D secretion profiles and clustered with PhenoGraph from three independent experiments **(I, II, and III)**. TAMs were isolated from end point (1 cm^3) tumors. TAMs that did not secrete any of the 15 measured targets above the detection limit were excluded from the analysis (~50%). Heat maps represent the fractions of cells in each cluster producing each of the 15 measured targets. Cluster names are based on the primary secreted target(s) in each cluster.

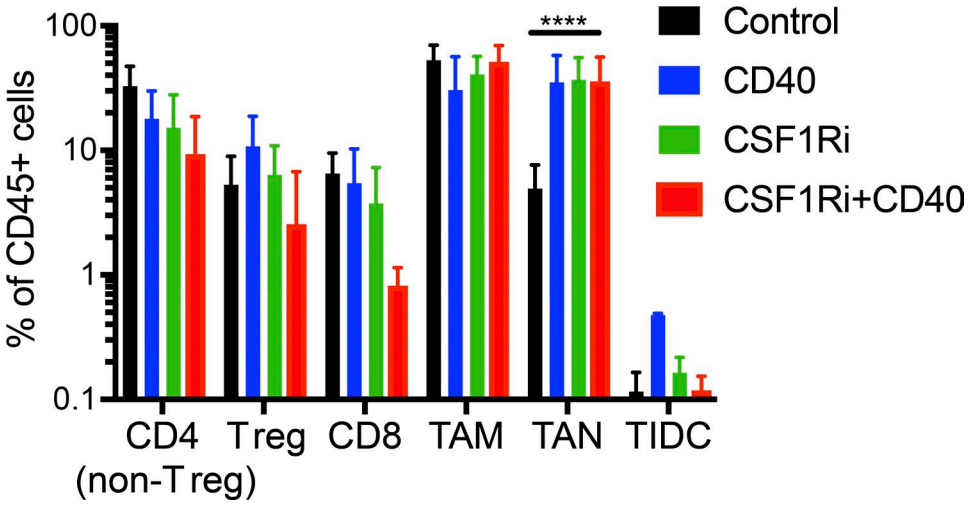

Figure S3. **Frequency of immune cell types.** Related to Fig. 3. Bar graphs show the percentage of total $CD45^+$ cells of infiltrating immune cell types (as indicated) in control tumors or those treated with CSF-1Ri, CD40, or the combination based on flow cytometry at the end point (day 60). Immune cell populations are defined as in Fig. 1 C. Data are from two independent experiments (n = 6–12) and are compared using one-way ANOVA with Holm-Sidak multiple comparisons correction. ****, $P < 0.001$.

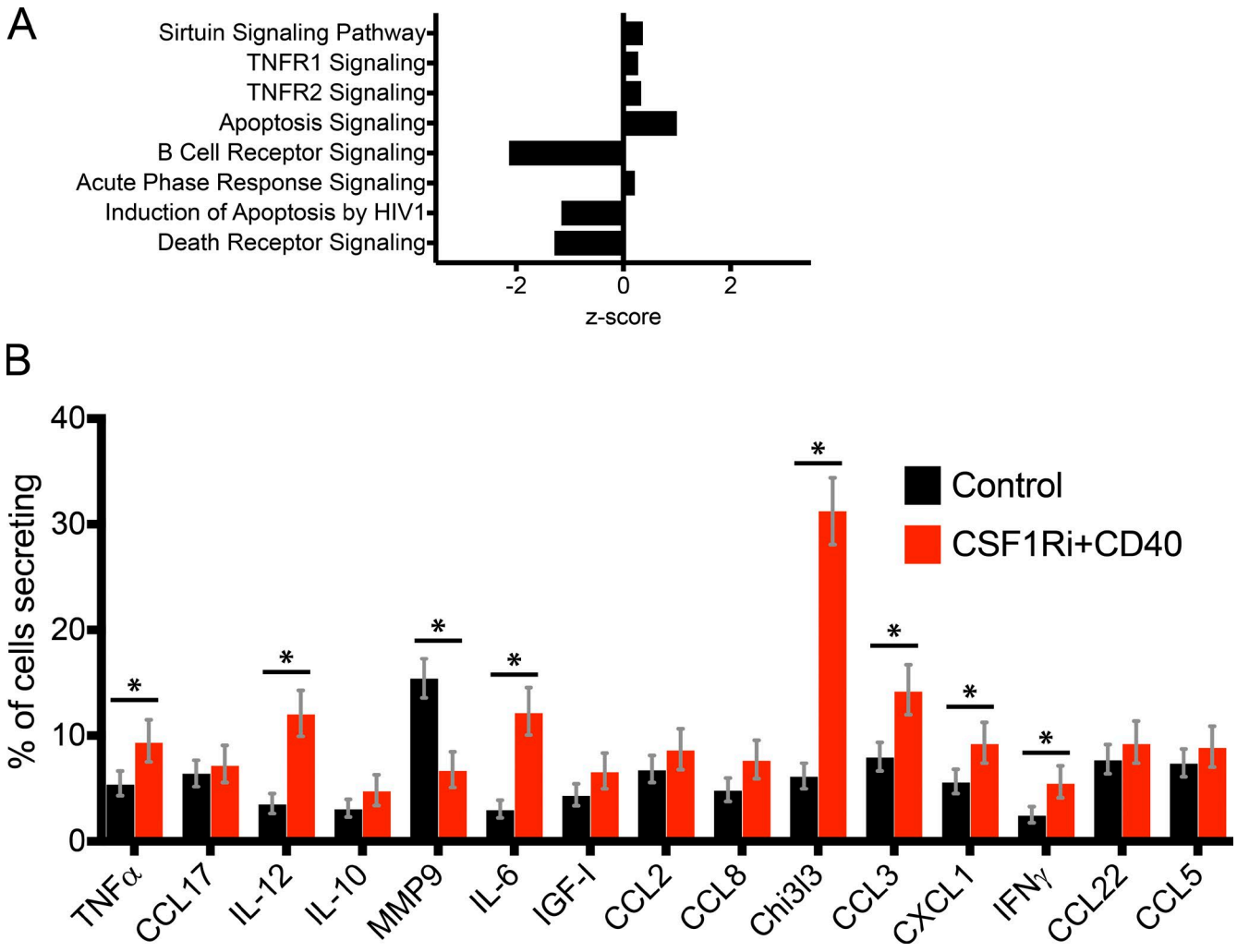

Figure S4. **Characterization of changes in TAM gene expression and secretion after CSF-1Ri+CD40 treatment.** Related to Figs. 4 and 5. **(A)** The top eight pathways in TAMs modulated by CSF-1Ri+CD40 treatment compared with control identified by ingenuity pathway analysis, sorted by ascending p-values. Pathway analysis was performed on genes that had an absolute log_2fold change >0.5 and an adjusted P <0.1. **(B)** Fractions of TAMs secreting each target from control versus CSF-1Ri+CD40-treated tumors at end point, 8 wk after tumor induction. Error bars represent the 95% confidence interval calculated by bootstrapping. *, P < 0.05.

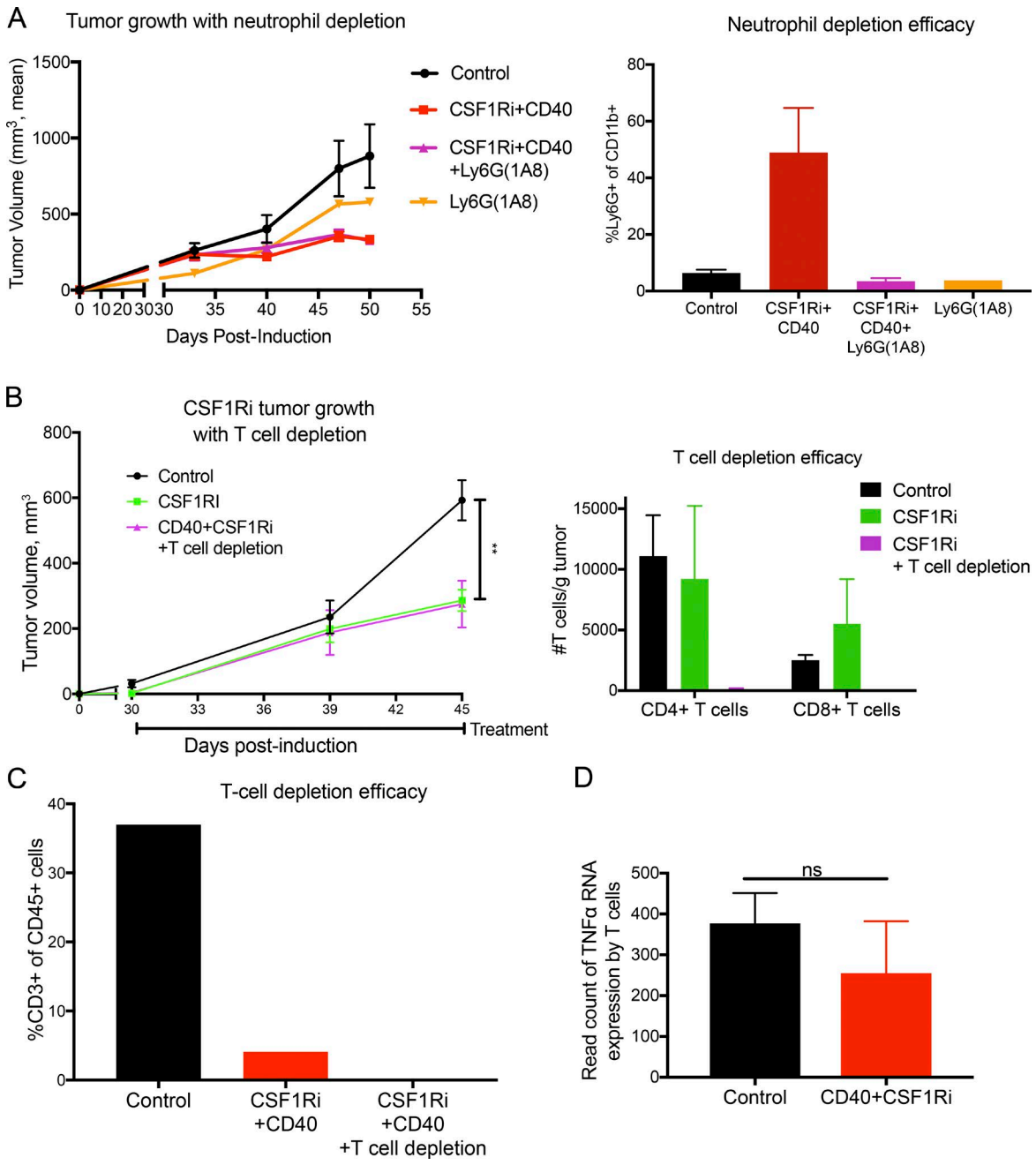

Figure S5. **Effect of neutrophils and T cells on efficacy of CSF-1Ri and CSF-1Ri+CD40 therapy.** Related to Fig. 6. **(A)** Tumor-bearing mice were treated with CSF-1Ri chow (600 mg PLX6134/kg chow) and CD40 agonistic antibody (10 mg FGK4.5 clone/kg every 3 d i.p.) with or without neutrophil-depleting antibody (20 mg 1A8/kg every 2 d i.p.) starting at day 30 after tumor induction until end point for a total of 10 treatments. TAN density in CSF-1Ri+CD40+1A8 was decreased by at least 97% compared with CSF-1Ri+CD40. Data are from one experiment and representative of two independent experiments ($n = 3$ each except Ly6G alone, for which $n = 1$). **(B)** Tumor-bearing mice were treated with CSF-1Ri chow (600 mg PLX6134/kg chow) starting at day 30 after tumor induction with 10 mg/kg anti-CD4 GK1.5 and 10 mg/kg anti-CD8 TIB210 every 3 d i.p. for a total of 10 treatments. Data are representative of two independent experiments. Suppression of Braf/Pten tumor growth by CD40 agonist monotherapy was previously shown to be T cell independent (Ho et al., 2014). **(C)** Braf/Pten mice were treated with CSF-1Ri (600 mg PLX6134/kg chow) and/or CD40 (10 mg FGK4.5/kg every 3 d) with or without T cell depletion (10 mg GK1.5 and TIB210/kg every 3 d) 30 d after tumor induction until end point (day 45) for a total of five treatments with FGK4.5 ± GK1.5/TIB210. Data are the mean percent $CD3^+$ of total $CD45^+$ cells from one experiment representative of two independent experiments with tumors combined from two to three mice per group. **(D)** *Tnf* transcription by $CD3^+$ T cells from control and CSF-1Ri+CD40-treated tumors from end point (day 60) as in Fig. 6 B, sorted in parallel with the TAMs in Fig. 4 A, with a sort layout outlined in Fig. S1 A. Sorted cells were $CD3^+/CD45^+/CD11b^-$/LiveDEAD$^-$. Data are from two or three independent experiments ($n = 2–3$ each group, with three individual tumors pooled for each sample). ns, not significant. **, $P < 0.01$.

REFERENCE

Ho, P.-C., K.M. Meeth, Y.-C. Tsui, B. Srivastava, M.W. Bosenberg, and S.M. Kaech. 2014. Immune-based antitumor effects of BRAF inhibitors rely on signaling by CD40L and IFNγ. *Cancer Res.* 74:3205–3217. https://doi.org/10.1158/0008-5472.CAN-13-3461